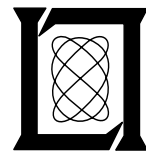# Air-to-Air Visual Acquisition Performance with TCAS II

J. W. Andrews

7 November 1984

Lincoln Laboratory
MASSACHUSETTS INSTITUTE OF TECHNOLOGY
LEXINGTON, MASSACHUSETTS

1. Report No.	2. Government Accession No.	3. Recipient's Catalog No.
DOT/FAA/PM-84/17		

4. Title and Subtitle	5. Report Date
Air-to-Air Visual Acquisition Performance with TCAS II	7 November 1984
	6. Performing Organization Code

7. Author(s)	8. Performing Organization Report No.
John W. Andrews	ATC-130

9. Performing Organization Name and Address	10. Work Unit No.
Lincoln Laboratory, M.I.T. P.O. Box 73 Lexington, MA 02173-0073	
	11. Contract or Grant No.
	DOT-FA77-WAI-817
	13. Type of Report and Period Covered

12. Sponsoring Agency Name and Address	
Program Engineering and Maintenance Service Department of Transportation Federal Aviation Administration Washington, D.C. 20591	Project Report
	14. Sponsoring Agency Code

15. Supplementary Notes

16. Abstract

The ability of pilots to visually acquire aircraft approaching on collision courses is analyzed using a mathematical model of visual acquisition. The model is calibrated by reference to subject pilot flight test data resulting from testing of the Traffic Alert and Collision Avoidance System (TCAS).

Techniques are presented that allow the determination of the probability of visual acquisition for a range of intruder aircraft sizes and closing rates. The effect of visual range (atmospheric visibility) upon visual acquisition performance is analyzed.

17. Key Words	18. Distribution Statement
TCAS traffic alert visual acquisition visual range	Document is available to the public through the National Technical Information Service, Springfield, Virgina 22161.

19. Security Classif. (of this report)	20. Security Classif. (of this page)	21. No. of Pages	22. Price
Unclassified	Unclassified	46	

Form DOT F 1700.7 (8-69)

SUMMARY

This report provides an analysis of air-to-air pilot visual acquisition performance for aircraft equipped with the Traffic Alert and Collision Avoidance System (TCAS). The analysis uses a model of air-to-air visual acquisition that was developed previously in flight testing at Lincoln Laboratory.

Model parameters are selected to reflect flight test experience with TCAS at Lincoln Laboratory. Techniques are presented that allow the determination of probability of visual acquisition for a range of aircraft types and closure rates.

Average probabilities of visual acquisition are presented for typical aircraft types. The model predicts that for aircraft on near-collision courses, timely visual acquisition will occur in 80-90 percent of the encounters. However, there are certain cases (e.g., head-on encounter with a small target) in which the probability of visual acquisition is less than 40 percent.

Appendix A presents techniques for predicting the effect of visual range (meteorological visibility) upon visual acquisition performance. It is shown that at higher closing rates, visual range can have a significant effect upon acquisition performance even though the visual range is above VFR minimums.

CONTENTS

ILLUSTRATIONS

APPENDIX ILLUSTRATIONS

TABLES

AIR-TO-AIR VISUAL ACQUISITION PERFORMANCE WITH TCAS II

1.0   INTRODUCTION

In 1982 the Federal Aviation Administration initiated a system safety study (Ref. 1) of the Traffic Alert and Collision Avoidance System II (TCAS II). The purpose of this study was to define the net safety benefits to be derived from the implementation of the TCAS and to determine the extent to which anamolous conditions (such as defective aircraft altimetry) could degrade system performance. In order to complete the study it was necessary to estimate the visual acquisition performance resulting from use of the automated traffic advisories provided by TCAS II. TCAS II displays automatic traffic advisories that depict the range, bearing, and relative altitude of selected nearby aircraft. Visual acquisition data for TCAS subject pilots was available for some 66 near-miss encounters that were flown as part of TCAS flight testing at Lincoln Laboratory (Ref. 2). This data was analyzed using a visual acquisition model developed at Lincoln Laboratory during testing of an earlier CAS concept (Ref. 3). This report provides the results of that analysis. It also includes an appendix that provides additional analysis of the effects of visual range upon acquisition performance.

The manner in which the Lincoln Laboratory visual acquisition model was derived and validated is described in Ref. 3. A brief summary of the key features of the model will be presented here. For further information on visual acquisition in aviation, the reader is referred to Refs. 4-14.

1

2.0 FUNDAMENTAL PROPERTIES OF THE MODEL

The ability of a pilot to visually acquire another aircraft varies greatly with the conditions of visual search. The visual acquisition model seeks to describe the acquisition process in terms of a visual acquisition rate, λ, that is defined as follows

$$\lambda(T) = \lim_{\Delta T \to 0} \frac{P[\text{acquisition between T and } T + \Delta T]}{\Delta T} \qquad (2.1)$$

In this model, visual acquisition is viewed mathematically as a non-homogenous Poisson process (i.e., a Poisson process in which the rate can vary with time). Typically a Poisson process is used to describe processes for which any number of discrete events can occur over a given time interval. In this case, the scope of the model is restricted to include only the possiblities of zero events (no acquisition) or one event (acquisition). The probability of visual acquisition can then be written

$$P[\text{acq by } T_2] = 1 - \exp\left[-\int_{-\infty}^{T_2} \lambda(T) \, dT\right] \qquad (2.2)$$

This mathematical formulation provides a powerful general framework for model development. Within this framework, modeling efforts are directed toward properly representing the value of λ for different search conditions.

Figure 2-1 depicts the functional relationships between various factors that influence the visual acquisition rate. It can be seen that the visual area (i.e., the target area normal to the line-of-sight) is a function of the target aircraft type and the aspect angle with which it is seen. The visual area together with the range determines the subtended solid angle of the target. For a non-maneuvering collision situation, the visual area is constant. The effective contrast of the target is determined by the range, the atmospheric absorption, and the inherent contrast of the target with the background. The subtended solid angle and the effective contrast together determine the detectability of the target. This detectability is related to the angular proximity that must exist between the target and the foveal center of the pilots search in order for acquisition to occur. The angular region within which detection can occur is sometimes called the "visual lobe". The fraction of time devoted to visual search and the angular area over which the search is conducted also impact the acquisition rate. And a target must be within the pilot's field-of-view in order to be acquired.
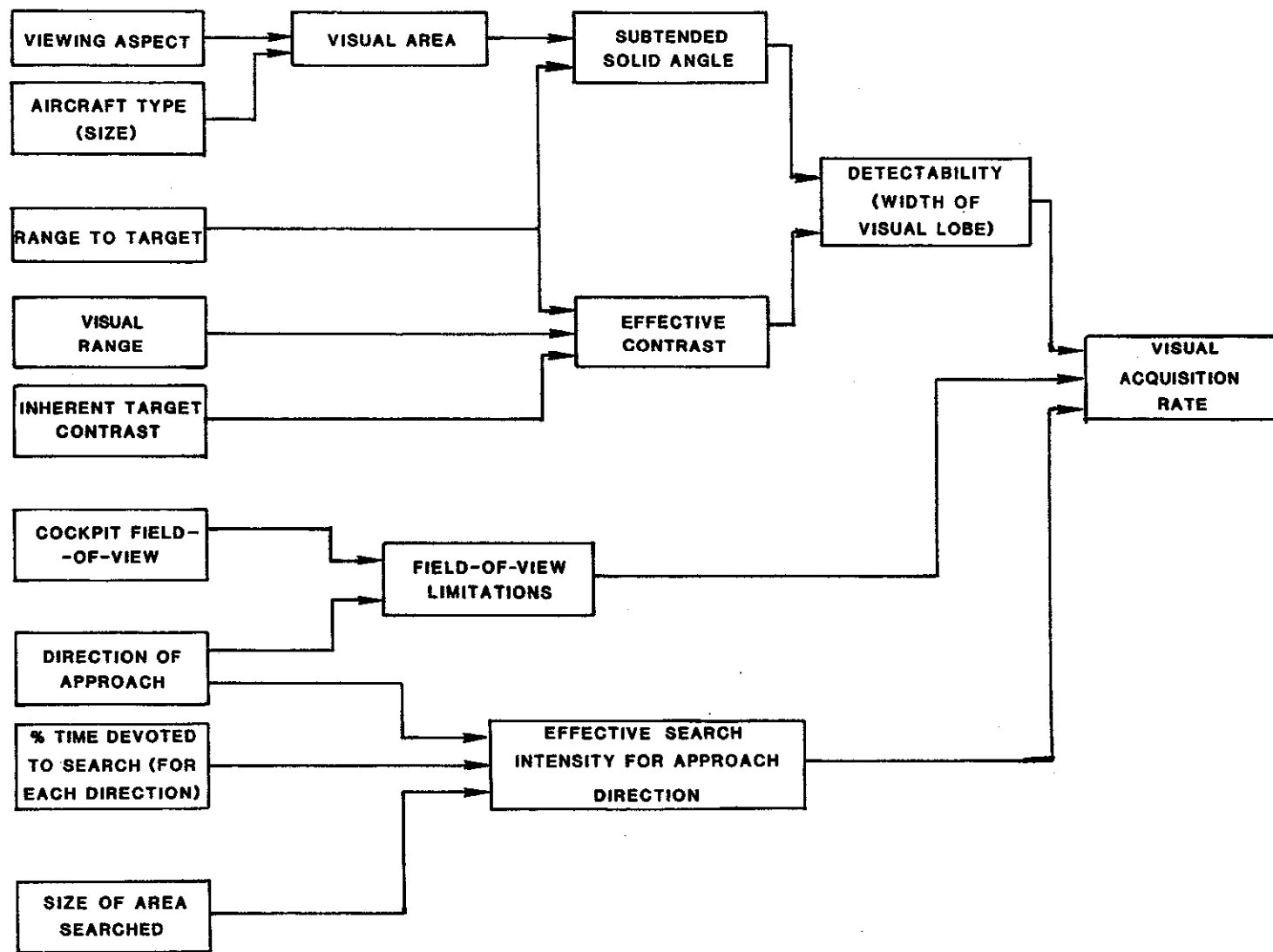
2

Fig. 2.1. Functional relationship between the factors that determine the visual acquisition rate at a particular instant of time.

Many complex and incompletely understood processes are associated with human vision in the flight environment. For example, it is possible for a pilot to "see" an aircraft against complex terrain features and fail to recognize the shape as an aircraft. It is possible for the pilot to suffer "empty field myopia" and fail to focus his eyes at a sufficient distance to acquire. It is also possible for special target properties such as sun glint, vapor trails, or aircraft angular motion relative to the background to assist in visual detection. A model which was elaborated to reflect all known or postulated subtleties of visual acquisition would soon flounder upon limitations of the theory and the need to accumulate an enormous data base in order to validate model parameters. The model employed here views visual acquisition as primarily a problem of visual detection. Flight test data is well-described using this approach. Subtle and complex effects are apparently either rare or else their statistical nature is compatible with the mathematical structure of the proposed model.

The principal mathematical relationship validated by flight test data (Ref. 3) is that under nominal search conditions the acquisition rate (i.e., probability of acquisition per unit of time) is proportional to the solid angle subtended by the target. The acquisition rate can then be written

$$\lambda = \beta \frac{A}{r^2} \tag{2.3}$$

(see Table 2.1 for explanation of notation).

The value of β that properly models the acquisition rate changes when the pilot receives a traffic advisory. If a value β_0 applies at all times prior to the traffic advisory and a value β_1 applies at all times after the traffic advisory, then the probability of visual acquisition is

$$p \begin{bmatrix} \text{acquisition} \\ \text{by } T_2 \end{bmatrix} = 1 - \exp \int_{-\infty}^{T_1} \frac{\beta_0 A}{r^2} dT + \int_{T_1}^{T_2} \frac{\beta_1 A}{r^2} dT \qquad T_2 > T_1 \tag{2.4}$$

For unaccelerated flight the range to the target is given by

$$r = (m^2 + v^2 t^2)^{1/2} \tag{2.5}$$

In all equations which follow we will express time in terms of time-to-closest approach, t. Note that t decreases with clock time according to the equation

$$dt = -dT \tag{2.6}$$

4

TABLE 2.1

NOTATION EMPLOYED IN VISUAL ACQUISITION ANALYSIS

A Aircraft visible area

A_x Aircraft visible area when viewed head-on (from 12 o'clock)

A_y Aircraft visible area when viewed broadside (from 3 o'clock)

A_z Aircraft visible area when viewed from directly above

m Horizontal miss distance

r Range between aircraft

$\dot{r}$ Range rate

t_1 Time at which alerted search begins (seconds before projected closest approach)

t_2 Time at which visual search terminates (seconds before closest approach)

V Speed of aircraft 2 relative to aircraft 1

V_1 Airspeed of TCAS aircraft (own aircraft)

V_2 Airspeed of intruder aircraft

β Model constant which relates acquisition rate to the subtended solid angle of the target aircraft

λ Acquisition rate (instantaneous probability of acquisition per instant of time)

θ_1 Bearing of aircraft 2 as seen from aircraft 1 (degrees clockwise from the 12 o'clock position)

θ_2 Bearing of aircraft 1 as seen from aircraft 2 (degrees clockwise from the 12 o'clock position)

χ Crossing angle (heading of aircraft 2 less heading of aircraft 1)

5

If A is constant, then equation (2.4) can be integrated to yield

$$p\;[\text{acquisition by } t_2] = 1 - \exp\;\frac{-\beta A}{Vm}\;(\arctan\frac{V\,t_1}{m} - \arctan\frac{V\,t_2}{m}) \qquad (2.7)$$

For an actual collision course, m=0 and $V = -\dot{r}$. The above expression then becomes

$$p\;[\text{acquisition by } t_2] = 1 - \exp\;[\frac{-A}{\dot{r}^2}\;(\frac{\beta_1}{t_2} - \frac{\beta_1 - \beta_0}{t_1})],\;t_1 > t_2 \qquad (2.8)$$

Normally the search effort which precedes the traffic advisory does not contribute greatly to the ultimate visual acquisition probability. This is true for two reasons: 1) unalerted visual search is relatively ineffective compared to alerted search ($\beta_0 \ll \beta_1$), and 2) at earlier times the target is at greater ranges and hence is more difficult to detect. It can be shown from equation (2.8) that search that takes place at more than 3 times the required acquisition time (t_2) contributes minimally to the ultimate probability of acquisition. (For the TCAS system, the traffic advisory appears at about 3 times the required acquisition time.) In the interest of simplicity, the following analysis will assume that no visual acquisition can occur prior to the traffic advisory (i.e., $\beta_0 = 0$). Equation (2.8) then becomes

$$p\;[\text{Acquisition by } t_2] = 1 - \exp\;[-\frac{\beta A}{\dot{r}^2}\;(\frac{1}{t_2} - \frac{1}{t_1})],\;t_1 \geq t_2 \qquad (2.9)$$

It can be seen that this expression takes the size of the target, the closing rate, and the time of alerted search into account in explicit fashion. Other factors must be taken into account by proper selection of the model constant β.

There is a theoretical basis for extending the model into cases in which atmospheric visibility significantly degrades visual acquisition capability. The technique for doing this is described in Appendix A. Other calculations in this report will be restricted to cases in which meteorological visibility does not significantly affect performance.

3.0 APPLICATION OF THE MODEL TO TCAS

Determination of the Model Constant

For the purpose of this analysis, it will be assumed that β is equal to zero (and hence that no visual acquisition is possible) under the following conditions:

- Instrument meterological conditions (IMC) exist.

- The target is outside the pilot's field-of-view.

- The pilot is unable to interrupt his other tasks in order to search for the target.

- The pilot has received a TCAS traffic advisory (TA) but has misunderstood or misinterpreted it.

These assumptions are conservative, since (with the exception of the field-of-view requirement) none of these conditions absolutely preclude visual acquisition. In addition, visual search prior to the TCAS TA sometimes results in early acquisition.

The value of β that applies to a given set of search conditions can be determined by experiment. Figure 3.1 provides visual acquisition data gathered during TCAS subject pilot flight tests at Lincoln Laboratory (Ref. 2). A table containing this data can be found in Appendix B. This data represents single-pilot alerted search in which the alerted period began approximately 40 seconds prior to closest approach. A value of β can be inferred from such data in several ways. In Ref. 2, the maximum likelihood estimator for β is shown to be

$$\hat{\beta} = \frac{N}{\sum_{i=1}^{n} A/r^2 \, dt} \tag{3.1}$$

where n is the number of encounters involved in the experiment and N is the number of times acquisition occurred. The range of the integral for each encounter is the interval (prior to acquisition) at which nominal search conditions prevailed.

Although this estimator is optimum under the assumptions used in its derivation, it can significantly underestimate β if only a few bad data point are included. For instance, if the input data includes an encounter for which the target aircraft moves outside the field of view, the integrated solid angle may become very large without visual acquisition occurring. This could result in a large unjustified increase in the denominator in equation 3.1. The data in Fig. 3.1 contains at least six encounters in which the intruder was not acquired before it flew out of sight, passing beneath the noise of the

7
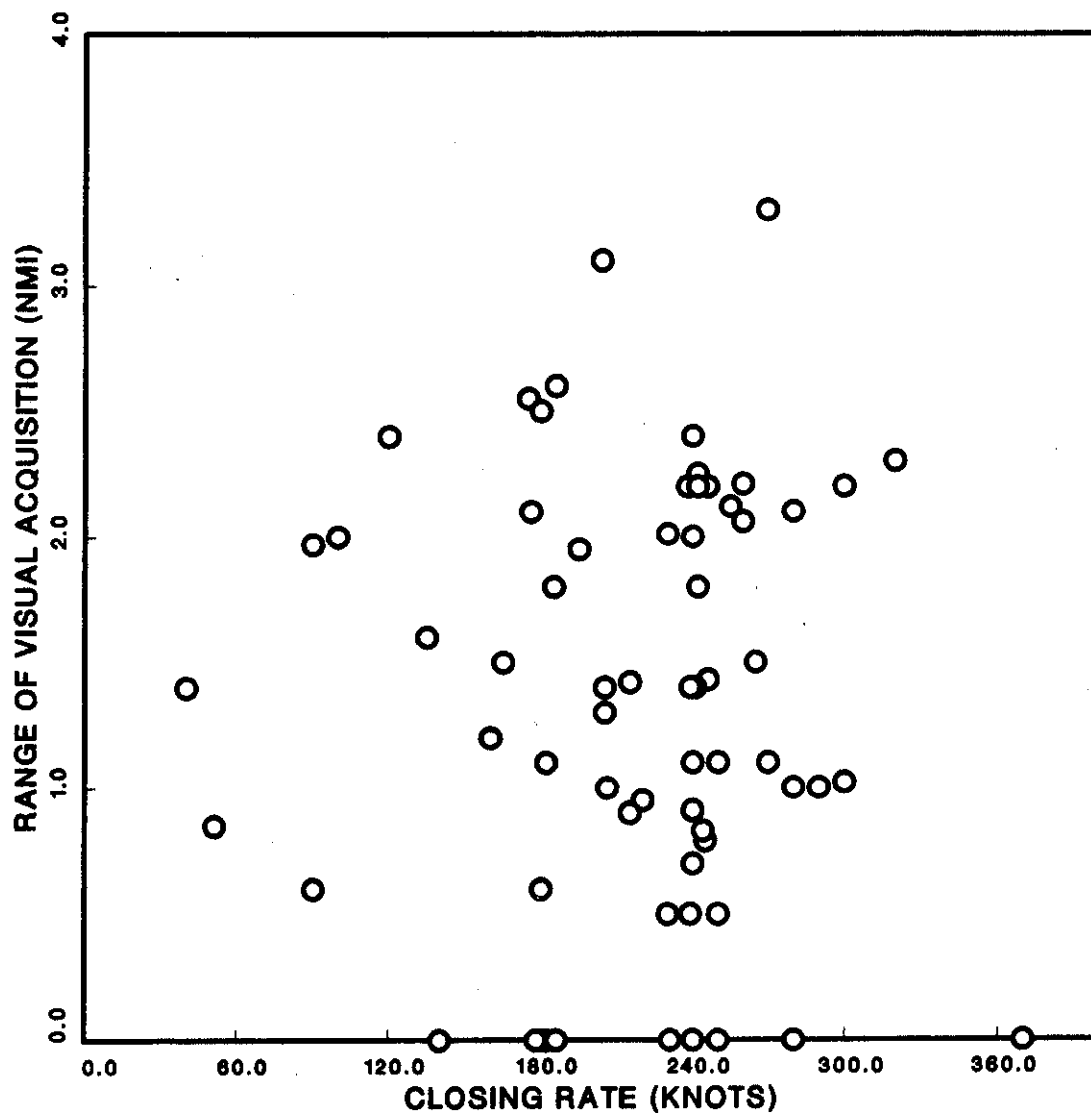
Fig. 3.1 Visual acquisition ranges versus closing rate for 66 subject pilot encounters. By convention, encounters with no visual acquisition are plotted at zero range.

8

TCAS aircraft that was climbing in response to a resolution advisory. Because the exact instant at which the intruder passed outside the field-of-view is unknown, the range of the integral to be used for these six encounters is uncertain.

Some of these data reduction difficulties can be alleviated by using a simpler and more robust estimator that selects the value of β that reproduces the median acquisition range of the data. This estimator can be written

$$\hat{\beta} = \frac{|\dot{r}| \ln 2}{A} \frac{r_1 r_2}{r_1 - r_2} \qquad (3.2)$$

where r_1 is the range at which search began and r_2 is the median acquisition range.

Although theoretically less accurate than the maximum likelihood estimator, this estimator is insensitive to the inclusion of a small number of non-nominal encounters in the data set. When this estimator is applied to the TCAS data, the median acquisition range of 1.4 nmi (at 250 knots closing rate and 40 square feet target area) yields a β estimate of 130,000/s. This value can be compared to the value of 90,000/s derived during testing of the ATARS traffic advisory system (Ref. 3). A higher value of β is to be expected for TCAS due to the higher accuracy of the TCAS bearing indication.

In Ref. 3 the value of β that applied to single-pilot unalerted search for VFR flights was estimated to be approximately 10,000/sec. This implies that the presence of the ATARS traffic advisory increased the acquisition rate by a factor of approximately 9. This is not reasonable since merely alerting the pilot to initiate visual search can double the amount of time devoted to visual search and informing him of the direction in which to search decreases the angular search area by a factor of four or five. The effect upon alarm rate is mutiplicative (i.e., twice the search time in one-fourth the area should increase the acquisition rate by a factor of 8). In the calculations that follow, an unalerted single-pilot search value of 10,000/sec will be assumed. This number should not be regarded as fully validated since the value of β for unalerted search is dependent upon the fraction of time the pilot devotes to visual search and the manner in which the pilot's search effort is distributed in angle. Extrapolation of unalerted search results from one type of operation to another may be inappropriate if these factors are different in the two regimes. Fortunately, alerted search performance should be largely independent of the type of flight environment since the pilot is told when and where to look.

It should be noted that the β value above was derived for use in equation 2.9 and that this equation does not explicitly model the effect of visual range. However the flight test data was gathered under limited visual ranges (typically 10-20 nmi). Thus, the value of β that best fits equation 2.9 to test results is decreased by the fact that the visual range was less than infinity. In the extended model (see Appendix A), visual range is explicitly included through use of a separate factor in the formula for the acquisition rate. A higher value of β (corresponding to search performance under infinite visual range) is then required to fit the data.

9

If more than one pilot is involved in the visual search, then the probability that at least one pilot will acquire is obtained by using a β value that is the sum of the β values for the individual pilots.

Calculation of Visual Area

The visual area, A, is a function of the target aircraft size, and the aspect angle with which the target is viewed. A simple technique for calculating an approximate visual area is described in Ref. 3. In that approximation, the target aircraft is modeled as if it were an object consisting of only three perpendicular planar surfaces corresponding to the silhouette of the aircraft when viewed head-on, broadside, and from directly above (see Fig. 3.2). Appropriate values for the areas of these three surfaces are provided in Table 3.1 for three representative types of aircraft. For the calculations which follow, it will be assumed that the target aircraft is viewed from the horizontal plane and hence that only A_x and A_y contribute to the visual area. The approximation first computes the visual areas that would be presented by each planar surface in the absence of shielding:

$$a_x = A_x \, |\cos \theta_2|$$

$$a_y = A_y \, |\sin \theta_2|$$

where θ_1 and θ_2 are bearings as shown in Fig. 3.3.

The actual visual area can be written as the larger of these two areas plus the fraction of the remaining area that is not shielded. The actual computation of the unshielded area would be quite complicated, so it is simply assumed to be 1/3 of the total area possible. This yields the following approximation:

$$A = \max \, (a_x, \, a_y) + 1/3 \, \min \, (a_y, \, a_x) \tag{3.3}$$

This approximation is without error when the aircraft is viewed along a principal axis.

Field of View Limitations

Visual acquisition is not possible if the intruder approaches from outside the field-of-view of the crew. Figure 3.4 provides a plot of the approach bearing of intruders as a function of crossing angle χ and speed ratio. It will be noted that if the intruder speed is less than or equal to own speed (the most likely situation for a TCAS-equipped aircraft), then the intruder must approach from the forward hemisphere. If the intruder is much faster than own aircraft, then for $\chi < 30°$ the direction of approach will be within 30° of the tail (6 o'clock) position and is unlikely to enter the field-of-view of either crew member. It should be noted that after receiving a TCAS TA, the crew members are likely to alter their position within the cockpit to achieve an unobstructed view in the direction of the approaching intruder. Hence the effective field-of-view with TCAS is greater than for an unalerted pilot who may conduct his visual search entirely from a single position within the cockpit.
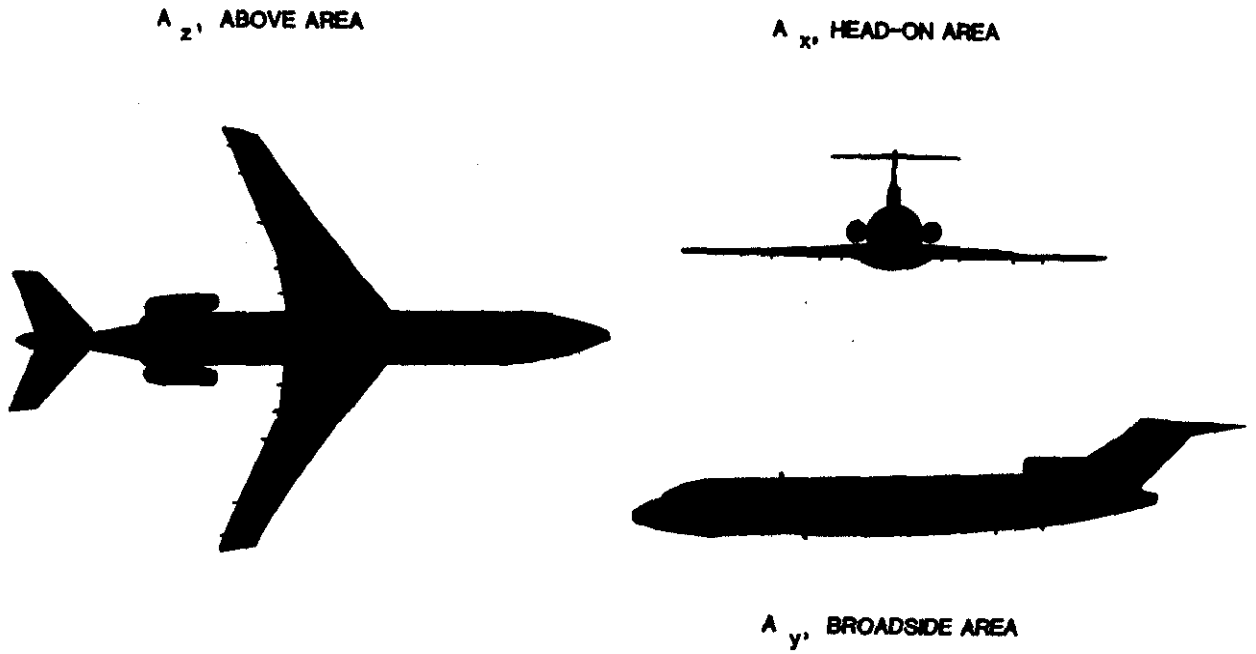
A$_z$, ABOVE AREA

A$_x$, HEAD-ON AREA

A$_y$, BROADSIDE AREA

Fig. 3.2 Principal target areas used to compute the
target visual area seen by the pilot.

TABLE 3.1

PRINCIPAL AREAS FOR THREE AIRCRAFT TYPES

Type Aircraft	Wingspan	Head-On Area, A_x	Broadside Area, A_y	Above Area, A_z
Single-Engine General Aviation (Cessna 182)	36 ft	35 ft^2	85 ft^2	260 ft^2
Multi-Engine Jet Transport (Boeing 727)	108 ft	400 ft^2	1900 ft^2	3100 ft^2
Military Jet Interceptor (McDonnell Douglas F-18)	45 ft	50 ft^2	280 ft^2	540 ft^2
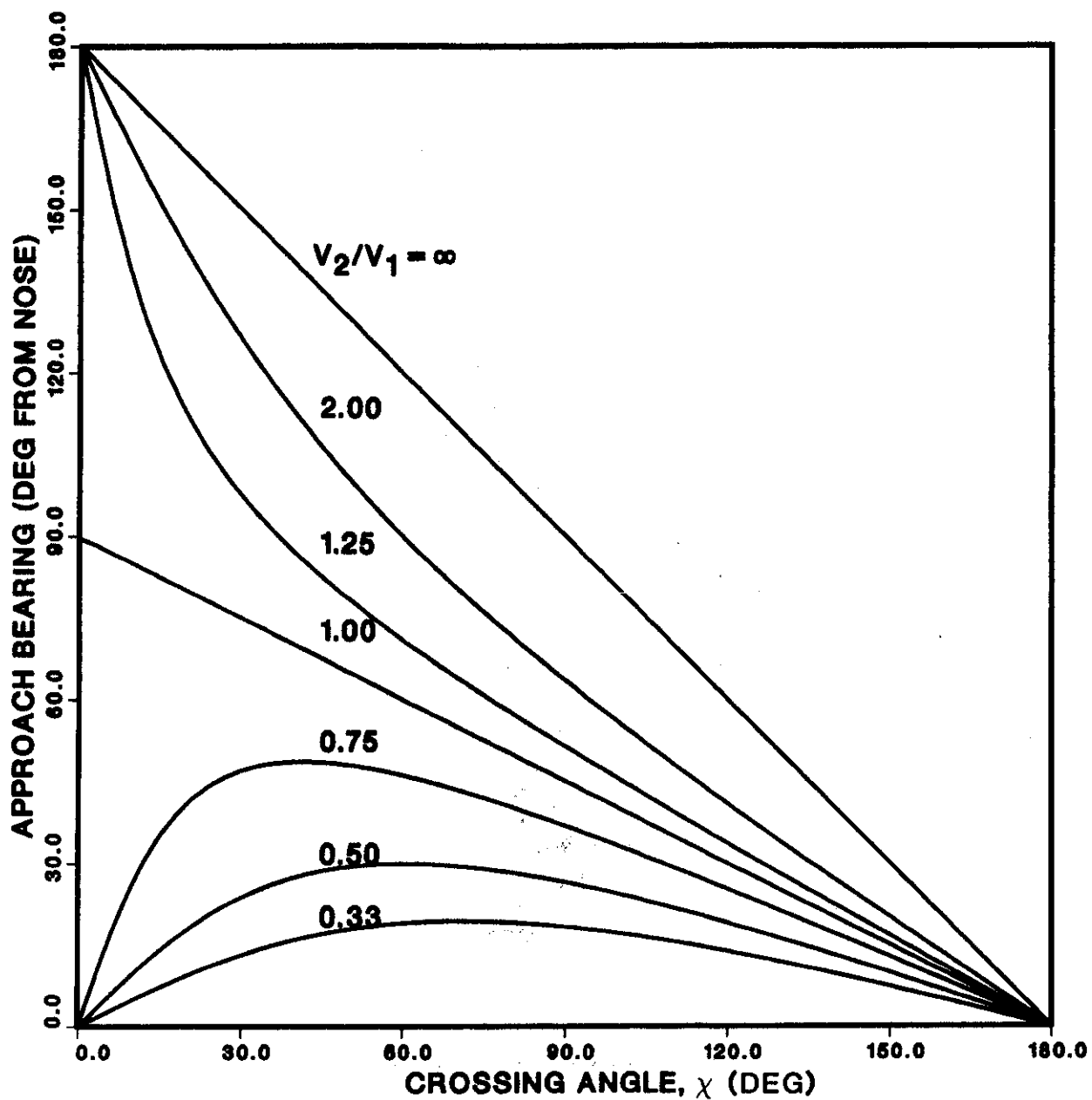
Fig. 3.4 Approach bearing of aircraft 2 as seen from aircraft 1.
Values are expressed in degrees from the nose (12 o'clock)
and assume rectilinear approach on a near-collision course.

Required Visual Acquisition Time

According to the model, when the target is approaching from within the field-of-view under nominal search conditions, the pilot is certain to acquire at some point since the angular size of the target will eventually become very large. But visual search must be regarded as unsuccessful unless acquisition occurs with enough lead time to allow the pilot to evaluate and react to the sighting. For most calculations it would be desirable to use the value of the acquisition lead time at which visual acquisition reduces the probability of collision by one-half. The failure rate for visual acquisition would then be computed by assuming that all acquisitions earlier than this time result in successful visual avoidance and that all later acquisitions result in failure. The failure rate thus computed would be a good approximation to the actual rate since the failures that occur despite earlier acquisition would be largely balanced by the successes that occur despite later acquisition.

Unfortunately there appears to be no definitive data on the amount of time required for visual avoidance. The TCAS system safety study (Ref. 1) used a value of 15 seconds. This value probably represents a reduction of much greater than a factor of two in the risk of collision. For military aircraft, it has been suggested (Ref. 14) that acquisition at only 5.5 seconds prior to collision is adequate for avoidance. In the calculations presented later, values of required acquisition time will be varied from 6 to 15 seconds.

Calculation of Visual Acquisition Probabilities

We will now calculate visual acquisition probabilities for some particular cases of interest. For these calculations it is assumed that the aircraft are approaching on an unaccelerated collision course with constant airspeeds. Let the crossing angle, χ, be defined as the difference in headings of the two aircraft (see Fig. 3.3). Thus $\chi = 0°$ corresponds to parallel flight and $\chi = 180°$ corresponds to a head-on encounter. χ can be written in terms of the bearings as follows:

$$\chi = \pi + \theta_1 - \theta_2 \tag{3.4}$$

A necessary condition for a collision course is

$$V_1 \sin \theta_1 + V_2 \sin \theta_2 = 0 \tag{3.5}$$

Taken together, these two equations define a unique pair of bearings which must exist for a collision to occur at a particular crossing angle. The range rate is then

$$\dot{r} = -V_1 \cos \theta_1 - V_2 \cos \theta_2 \tag{3.6}$$

The probability of visual acquisition before 15 seconds is given by equation (2.9) with t_2 = 15 seconds. Table 3.2 provides an example of the values of the relevant quantities for crossing angles from 0 to 180 degrees when the TCAS aircraft has an airspeed of 250 knots and the intruder is a small aircraft with an airspeed of 130 knots. Note that the acquisition probability is greater at shallow crossing angles when the closing rate is smaller. It decreases to a minimum in the head-on geometry.

Acquisition Performance Plots

A figure will now be presented which provides graphic delineation of the conditions under which visual acquisition can be achieved with confidence. The first step in developing such a figure is to note that if own airspeed and intruder type (see Table 3.1) are specified, then for each possible crossing angle there is a unique value of closing rate and target area. The loci of the target area/closing rate values are plotted in Fig. 3.5 with square symbols marking each 10 degree increment in χ. Note that the point for χ = 180° corresponds to observing the head-on area, A_χ, with a closing rate equal to the sum of the airspeeds of the two aircraft. If aircraft airspeeds are unequal, then χ = 0° corresponds to the faster aircraft overtaking the slower from behind. If airspeeds are equal, then χ = 0° corresponds to an infinitely slow convergence of aircraft on parallel flight paths.

Equation 2.9 can now be solved to determine the target area that would be required at a given closing speed to produce a specified probability of acquisition by t_2 seconds to closest approach. The result is

$$A(p) = \frac{\ln\left[\dfrac{1}{1-p}\right]}{\beta\,(1/t_2 - 1/t_1)}\; \dot{r}^2 \qquad (3.7)$$

where A is the required target area, p is the required probability of acquisition, and other variables are as defined previously. In Fig. 3.5 a family of curves is generated for various values of p. The value of β used corresponds to two-pilot alerted search, the nominal TCAS condition. The following conclusions can be drawn from this figure:

For a jet transport intruder, all possible encounter geometries lie within the region of high confidence in visual acquisition. For the smaller aircraft, the possible geometries are within the high-confidence region for lower crossing angles (χ < 90°) but pass out of the high-confidence region for higher crossing angles. In the worst case (χ = 180°), the probability of acquiring the smaller aircraft is less than 60 percent.

16

TABLE 3.2

CALCULATION OF VISUAL ACQUISITION PROBABILITIES - AN EXAMPLE

Own Airspeed: 250 knots
Intruder Airspeed: 130 knots
Intruder Size: A_x = 35 sq. ft. A_y = 85 sq. ft.
Time Search Begins: t_1 = 40 sec
Time at Which Visual Required: t_2 = 15 sec
Model Constant: β = 130,000/sec

X (deg)	θ_2 (deg)	θ_1 (deg)	$\dot{r}$ (kt)	A (sq. ft.)	P[acq]
0.0	180.0	0.0	-120.0	35.0	0.990
10.0	159.5	-10.5	-124.0	42.7	0.995
20.0	140.8	-19.2	-135.4	62.7	0.999
30.0	124.7	-25.3	-152.0	76.5	0.998
40.0	110.9	-29.1	-172.1	83.6	0.995
50.0	99.1	-30.9	-194.0	85.8	0.987
60.0	88.7	-31.3	-216.6	85.2	0.968
70.0	79.3	-30.7	-239.1	85.7	0.942
80.0	70.6	-29.4	-261.0	84.1	0.904
90.0	62.5	-27.5	-281.8	80.8	0.856
100.0	54.8	-25.2	-301.1	76.2	0.798
110.0	47.5	-22.5	-318.8	70.5	0.733
120.0	40.3	-19.7	-334.5	63.9	0.662
130.0	33.4	-16.6	-348.1	56.5	0.588
140.0	26.6	-13.4	-359.4	48.4	0.510
150.0	19.8	-10.2	-368.4	42.5	0.449
160.0	13.2	-6.8	-374.8	40.5	0.422
170.0	6.6	-3.4	-378.7	38.0	0.396
180.0	0.0	0.0	-380.0	35.0	0.369

Average (unweighted) = 0.766
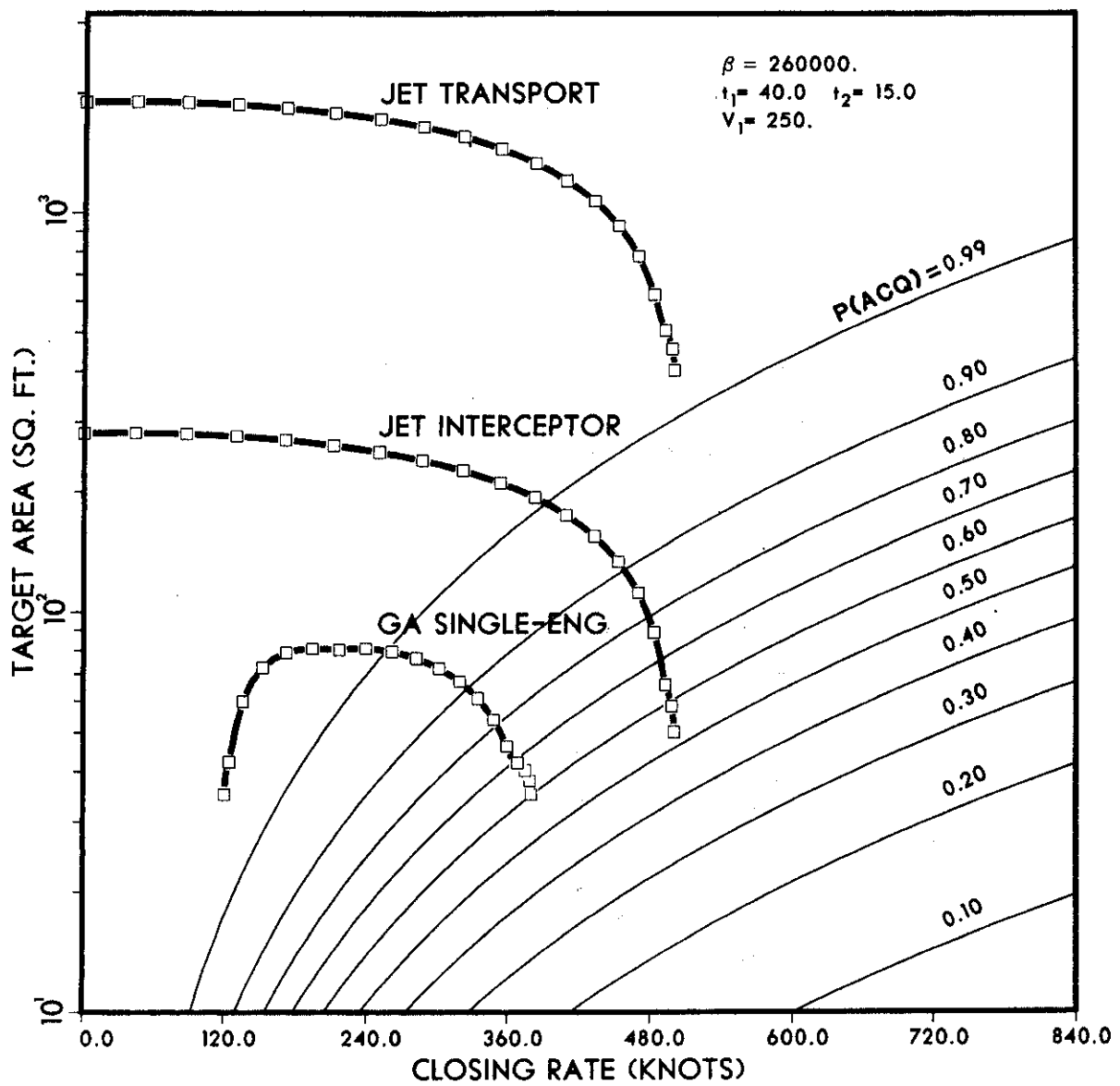
Fig. 3.5 Visual acquisition performance for parameter values typical of two-pilot alerted search.

Figure 3.6 is identical to Fig. 3.5 except that the value of β employed for the equal probability contours is 130,000/sec, a value that is representative of single-pilot search. Figure 3.7 illustrates the sensitivity of visual acquisition performance to variation in the value of the parameter β. The probability contours in this figure correspond to 90% probability of acquisition for β values that are multiples of 130,000/sec. Figure 3.8 provides curves for higher values of airspeed (corresponding to jet cruise regimes). Figure 3.9 provides curves for a required acquisition time (t_2) of 6 seconds.

Average Acquisition Probabilities

Certain parts of the TCAS system safety study require the use of an average probability of visual acquisition. In averaging acquisition probabilities, the values for each geometry should be weighted according to the likelihood with which that geometry occurs. If the heading of each aircraft is uniformly distributed between 0° and 360°, then all crossing angles are equally likely. For two aircraft selected at random, a uniformly weighted averaging of the values in Table 3.3 would then provide the average probability of visual acquisition for the pair. However, if aircraft are allowed to encounter each other in an unstructured fashion there will be more encounters with aircraft which are flying at higher speeds relative to the TCAS aircraft. In this case the average should be weighted according to relative speed. Because historic records of mid-air collisions involving air carrier aircraft reveal no trend toward particular geometries, an unweighted average over all crossing angles will be employed in the calculations which follow.

Table 3.3 provides the average probabilities of visual acquisition for a combination of airspeeds and intruder types.

Visual Acquisition Prior to RA

The probability that the crew of the TCAS aircraft will visually acquire the intruder prior to the appearance of the RA can be evaluated by setting t_2 equal to the time of RA generation, nominally 25 seconds to closest approach. Performance curves for this value of t_2 are provided in Fig. 3.10. It can be seen that the acquisition probability is quite high (over 95%) for the jet transport intruder. For the smaller aircraft, the probability varies with crossing angle. On average, visual acquisition occurs before the RA about half the time for smaller aircraft.

Relative Improvement in Acquisition Probability

A general description of the extent to which a change in the value of the parameter β can affect acquisition probabilities can be derived by using equation (2.9) to obtain:

$$q_1 = q_0^{\beta_1/\beta_0} \qquad (3.8)$$

19
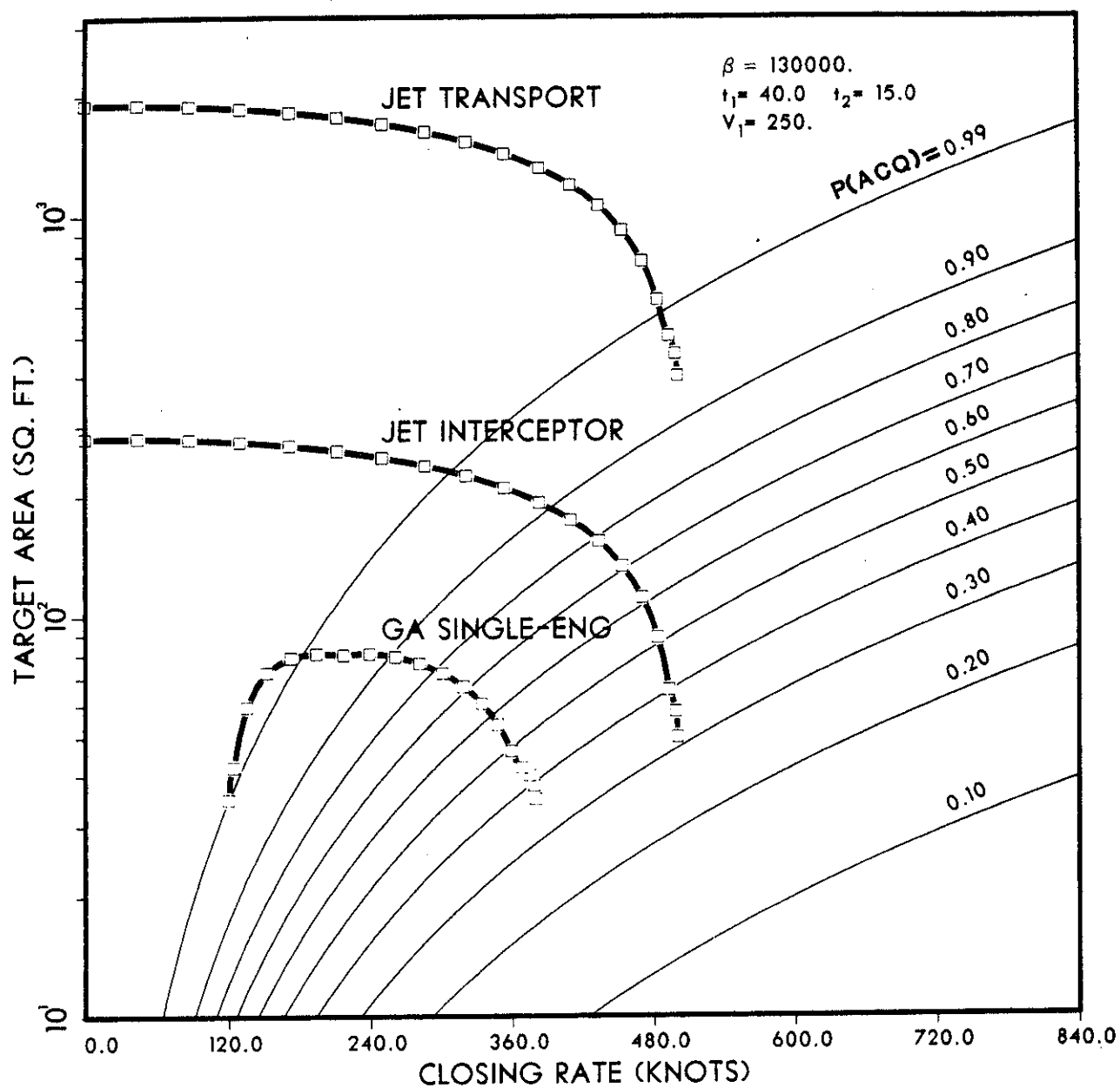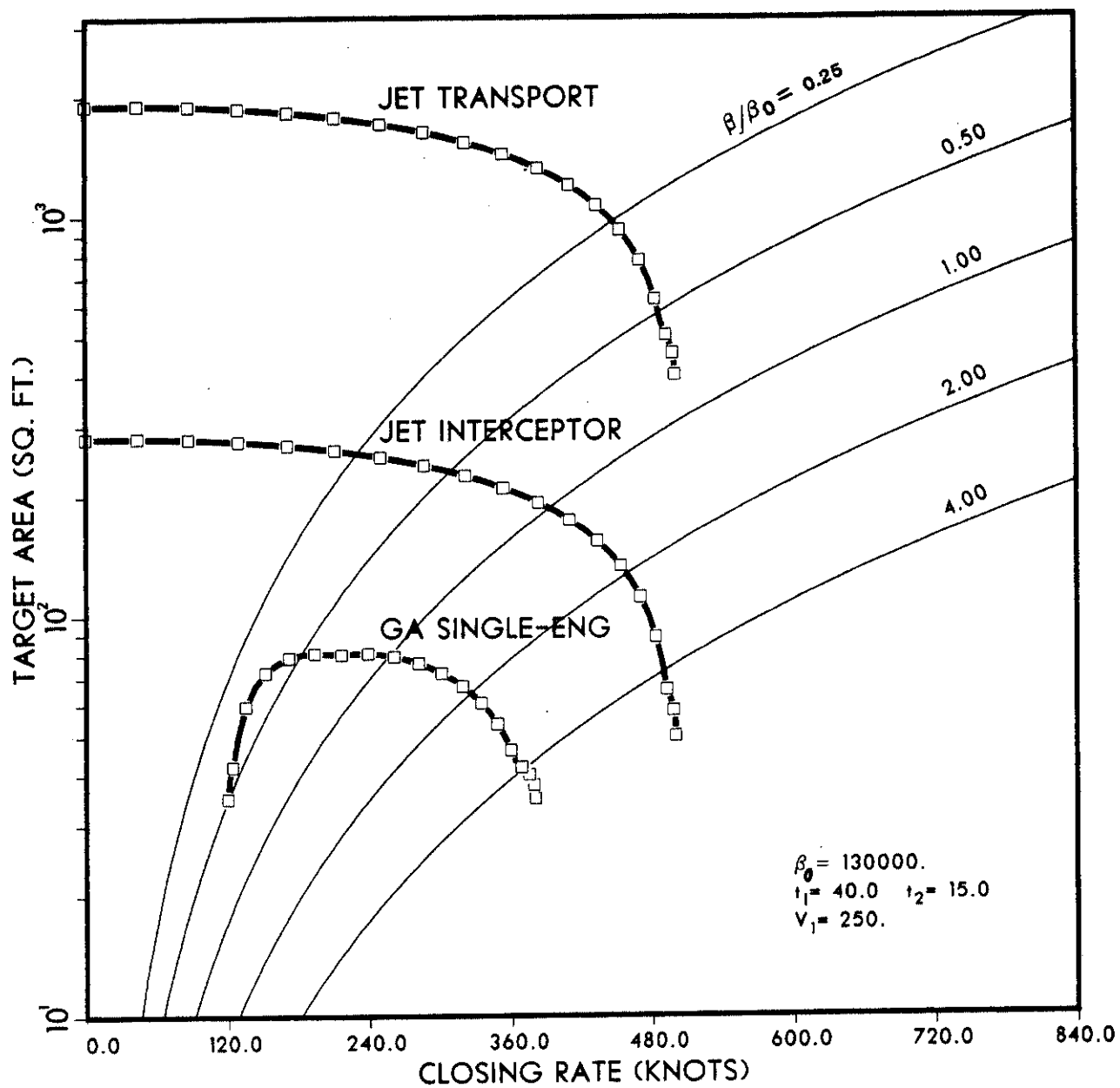
Fig. 3.6 Visual acquisition performance for parameter values typical of single -pilot alerted search.

Fig. 3.7 Effect of variations in β upon visual acquisition performance
Each contour is for 90 per cent probability of visual acquisition
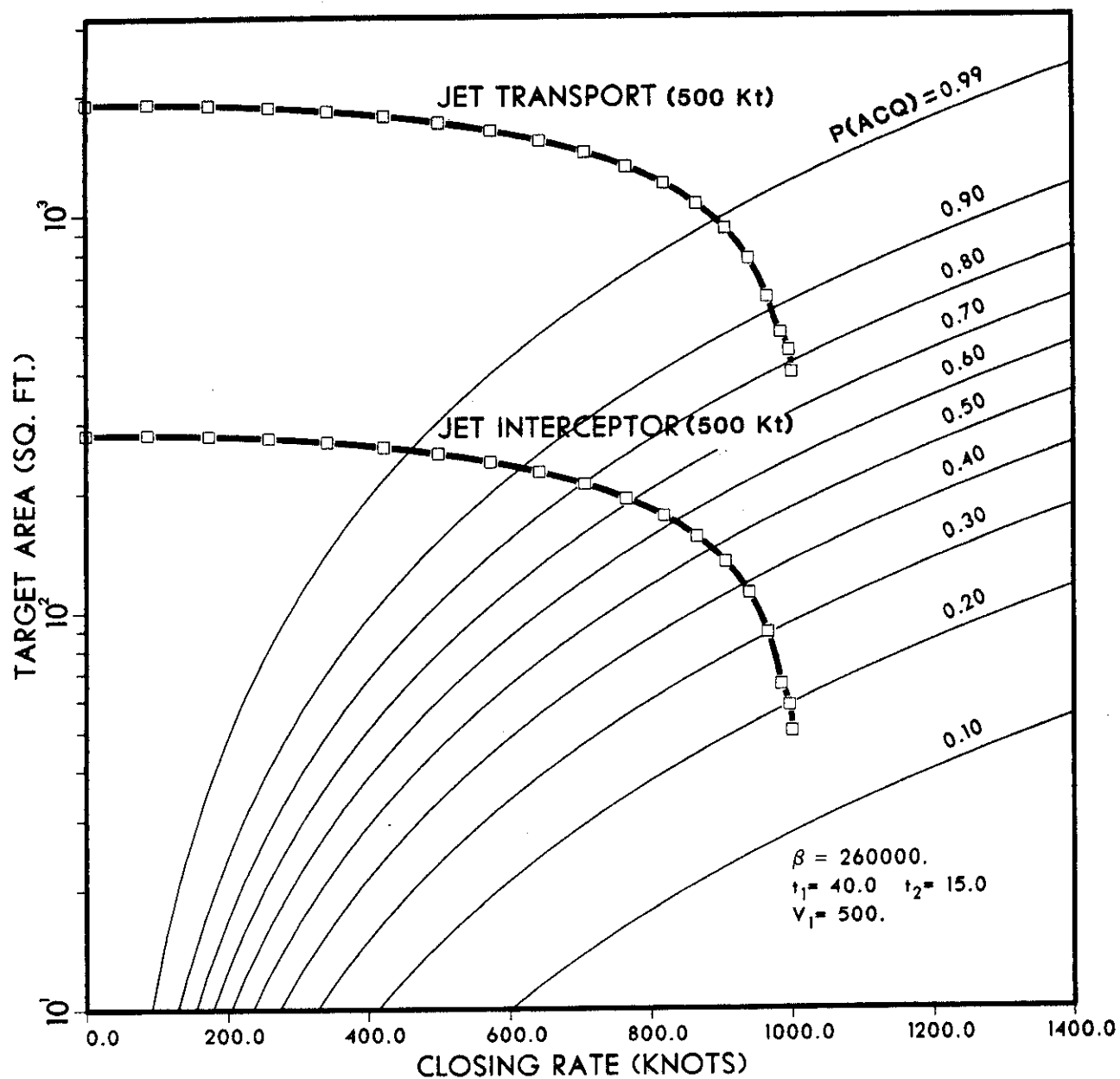at 15 seconds to CPA. The reference value of β is 130000/sec.

Fig. 3.8   Visual acquisition performance in a high speed
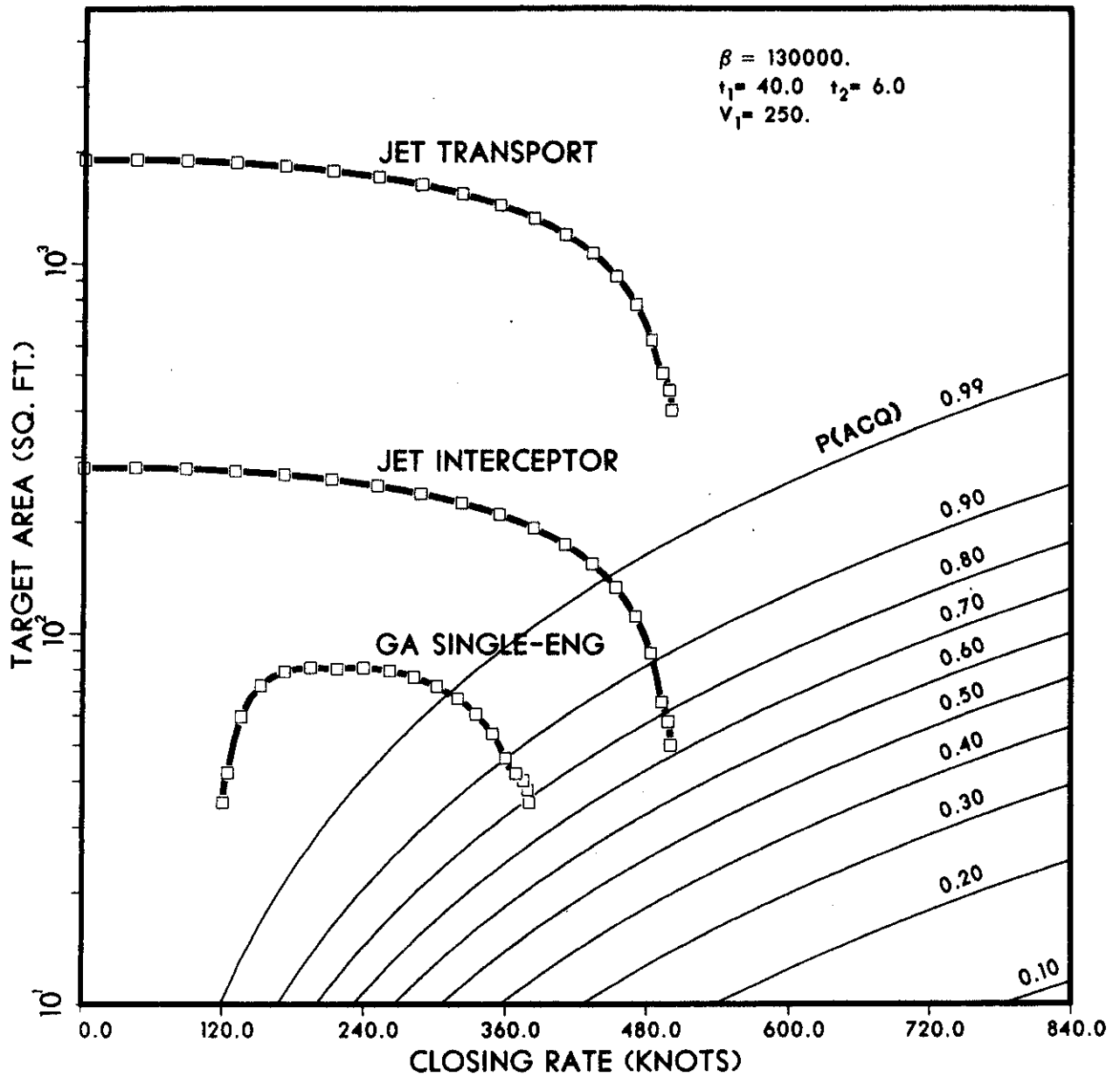regime (own airspeed 500 knots).

Fig. 3.9 Visual acquisition performance at 6 seconds before projected
collision for parameter values typical of single-pilot alerted search.

TABLE 3.3

AVERAGE PROBABILITIES OF VISUAL ACQUISITION

Search Start Time:	t_1 = 40 sec
Required Acquisition Time:	t_2 = 15 sec
Model Constant:	β = 130000. (single pilot, alerted)
	β = 260000. (two pilots, alerted)
	β = 20000. (two pilots, unalerted)

Own Airspeed (kt)	Intruder Type*	Intruder Airspeed (kt)	Intruder Size (sq. ft.)		P[Visual Acquisition]		
			A_x	A_y	Single Pilot, Alerted	Two Pilots, Alerted	Two Pilots, Unalerted
130	GA	130	35	85	0.890	0.969	0.534
180	GA	130	35	85	0.840	0.940	0.471
180	GA	180	35	85	0.775	0.896	0.421
250	GA	130	35	85	0.766	0.891	0.305
250	GA	180	35	85	0.716	0.847	0.347
250	JT	250	400	1900	0.994	1.000	0.828
500	JT	500	400	1900	0.896	0.965	0.584
250	MIL	250	50	280	0.812	0.907	0.488
500	MIL	500	50	280	0.572	0.695	0.293

*GA = General Aviation, single engine, JT = Jet Transport,
MIL = Military, jet interceptor.

24
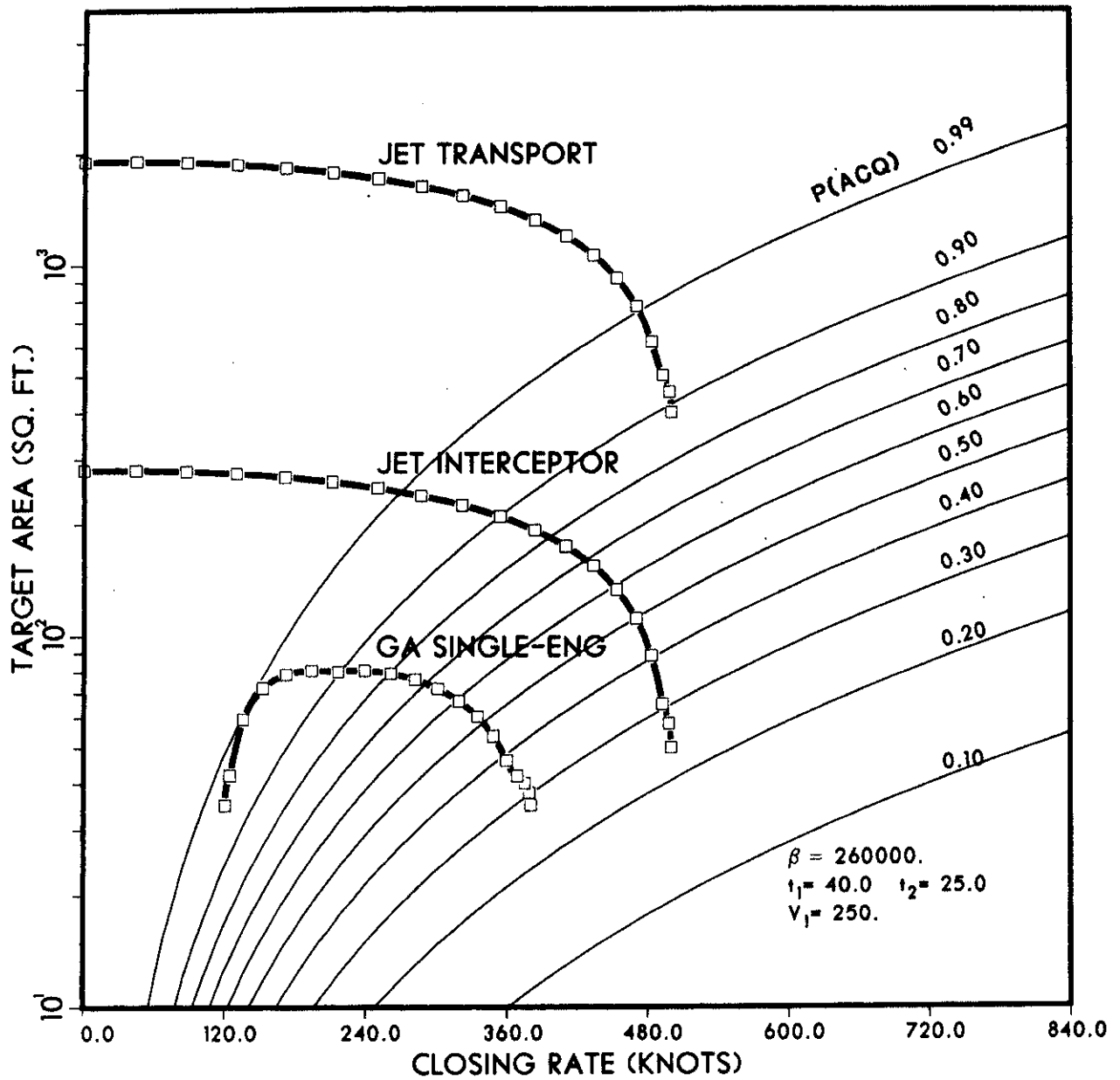
Fig. 3.10 Visual acquisition performance at 25 seconds
before projected collision (two-pilot alerted search).

where q_1 and q_0 are the probabilities of late acquisition for parameter values β_1 and β_0 respectively. Note that this relationship is independent of the target area, closing rate, or time of search. A plot of q_1 versus q_0 is provided in Fig. 3.11 for various ratios of β. This figure shows that when the probability of failure is originally fairly low (q_0 small), the presence of a traffic advisory should further decrease the failure rate by serveral orders of magnitude. When the probability of failure is high (q_0 near unity), then the addition of the traffic advisory may have minimal effect upon the final probability of success. This argues that traffic advisories may make visual acquisition highly reliable in cases where it already works fairly well, but cannot make visual acquisition reliable in cases where it is originally ineffective.

General Conclusions

The following general conclusions concerning visual acquisition are supported by the analysis presented in this chapter:

1) Under nominal search conditions, a TCAS II traffic advisory can increase the instantaneous rate of visual acquisition by an order of magnitude or more over the rate existing without an alert. The final visual acquisition probability is increased by a similar factor when it is initially very low ($p < 0.05$). The acquisition failure rate is decreased by a similar factor when the failure rate is initially moderate (less than 0.5).

2) In typical TCAS use there will remain a small percentage of situations in which visual acquisition is very difficult or impossible. These include flight in IMC, cases in which the intruder is not within the field-of-view, cases in which the crew misunderstands or misinterprets the traffic advisories, etc.

3) Against jet transport intruders at slower speeds (including all speeds likely below 10,000 feet altitude) visual acquisition is achieved with high confidence whenever nominal search conditions prevail. The predominant failure mode under these conditions will be the occurrence of non-nominal cases mentioned in 2) above.

4) Against smaller intruder types (small propeller aircraft and military interceptors) at lower altitudes, the likelihood of visual acquisition depends strongly upon the geometry of the intercept. On average, visual acquisition is expected in 80 to 90 percent of the encounters.

5) At jet cruise speeds, the probability of visual acquisition is strongly dependent upon the closing rates. At lower crossing angles ($\chi < 50°$), visual acquisition is achieved with high confidence against all types of intruders. However, for head-on geometries ($\chi = 180°$) the visual acquisition rate is expected to be approximately 70 percent for jet transport intruders and 15 percent for jet interceptor intruders.
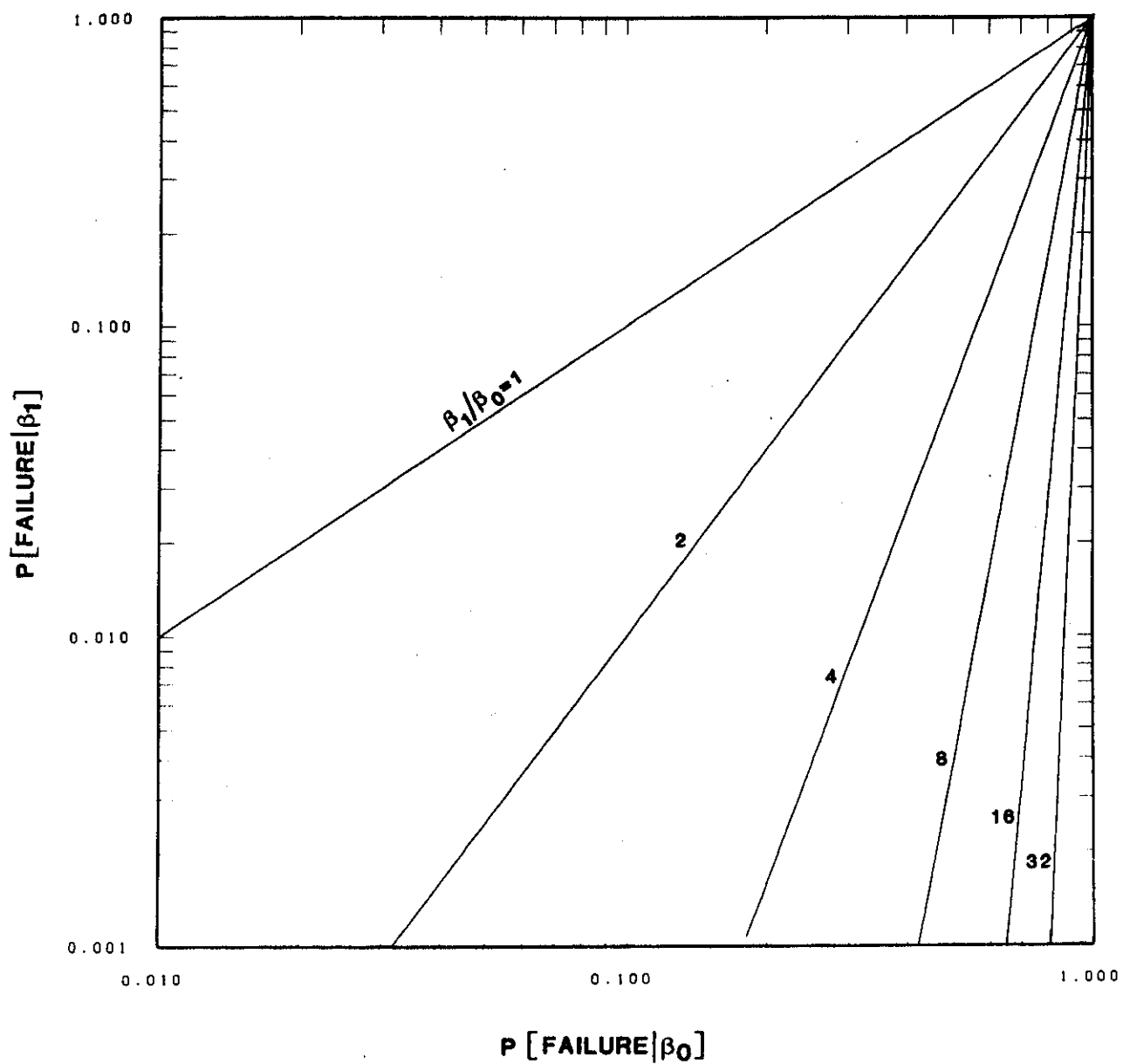
REFERENCES

1. Lebron J.E., _et.al._, "System Safety Study of Mimimum TCAS II," DOT/FAA/PM-83-36, The MITRE Corporation (December 1983).

2. Andrews, J.W., "Flight Testing of TCAS II with Subject Pilots," IEE Colloquium on Airborne Collision Avoidance-TCAS, Digest No. 1984/24 (5 March 1984).

3. Andrews, J.W., "Air-to-Air Visual Acquisition Performance with Pilot Warning Instruments (PWI)," Project Report ATC-73, FAA-RD-77-30, Lincoln Laboratory, M.I.T. (25 April 1977).

4. Greening, Charles P., "Mathematical Modelling of Air-to-Ground Target Acquisition," Human Factors, Vol. 18, No. 2 (April 1976).

5. Jones, Daniel B., "Air-to-Ground Target Acquisition Source Book: A Review of the Literature," AD-A015 079, Martin Marietta Aerospace (30 September 1974).

6. Hoffmann, H.E., "A Review of the Most Important Established Facts About the Visibility (Maximum Detection Range) of Aircraft," (RAE Library Translation No. 1895 from Deutsche Luft and Raumfahrt DLR-Mitt. 74-33, 1974).

7. Sulzer, R.L., and Skelton, G.E., "Visual Attention of Private Pilots, The Proportion of Time Devoted to Outside the Cockpit," Federal Aviation Administration (NAFEC), FAA-RD-76-80 (1980).

8. Lamar, E.S., Hecht, Schlaer, S. Hendley, C.D., "Size, Shape, and Contrast in Detection of Targets by Detection of Targets by Daylight Vision," Journal of the Optical Society of America, Vol. 37, No. 7 (July 1974).

9. Howell, W.D., "Determination of Daytime Conspicuity of Transport Aircraft," CAB-TDR-304, Civil Aeronautics Administration (May 1957).

10. Millhollon, A., Lyons, Graham, W., "Air-to-Air Visual Detection Data," Control Data Corporation, Interim Report, FAA-RD-73-40 (April 1973).

11. Graham, W. and Mangulis, V., "Results of the Visual Detection Simulation Experiment for the Evaluation of Aircraft Pilot Warning Instruments (APWI)," Control Data Corporation, Dec. FAA-RD-75-59, II (December 1974).

12. Rich, P.H., Crook, W.G., Sulzer, R.L., and Hill, P.R., "Reactions of Pilots to Warning Systems for Visual Collision Avoidance," National Aviation Facilities Experimental Center (FAA), FAA-NA-71-54 (December 1971).

13. Graham, W., and Orr, R.H., "Separation of Air Traffic by Visual Means: An Estimate of the Effectiveness of the See-and-Avoid Doctrine," Proceedings of the IEEE, Vol. 58, No. 3 (March 1970).

14. Wulfeck, J.W., Weisz, A., and Raben, M.W., "Vision In Military Aviation," WADC Technical Report 58-399 (ASTIA Doc. No. AD207780) (November 1958).

APPENDIX A

EFFECT OF METEOROLOGICAL VISIBILITY UPON VISUAL ACQUISITION

Meteorological visibility fundamentally impacts all areas of aviation that are dependent upon vision outside the cockpit. A model of visual acquisition performance would be much more complete if it could be used to predict pilot performance in fog and haze as well as in clear air. Development of such model capability is made difficult by the lack of flight test data concerning the impact of atmospheric visibility upon air-to-air visual acquisition performance. However, laboratory research provides a sound theoretical basis for extending the model previously described into situations of limited visibility. Such an extension and the results it produces are described below.

Haze and fog produces attenuation and scattering of light between the pilot's eyes and the target. The primary result of this upon the visual characteristics of the target is a lowering of the contrast between the target and its background. A standard formula for the contrast degradation (known as Koschmieder's Law) allows the contrast at range r to be written

$$C(r) = C_0 \ \exp\left[-2.996 \ \frac{r}{R}\right] \tag{A.1}$$

where C_0 is the inherent contrast (i.e., the contrast that would exist with no atmospheric attenuation or scattering over the line of sight) and R is the visual range (defined as the range at which the contrast of the target is decreased to 5 percent of C_0).

A brief explanation of the term visual range is in order here. In aviation, the visual range is usually defined as the greatest distance at which a large object (such as a runway) can be seen along a specified path (e.g., in the direction of landing). Studies have shown that this distance corresponds approximately to the point at which contrast has degraded to 5 percent of the inherent contrast. The World Meteorological Organization recommends that transmissometers be calibrated to report daylight visual range as the 5 percent range. For historical reasons, transmissometers in the U.S. are calibrated to 5.5 percent. In reading meteorological literature, one often encounters the meteorological optical range, defined as the range at which contrast has degraded to 2 percent. Reference A.2 contains a full discussion of these points. In the calculations presented here, the 5 percent definition will be used.

Studies of the impact of contrast upon visual detection (Ref. A.1) have shown that the detectability of small targets (1 to 10 min of arc) is dependent upon the product of the target area and its contrast. This is an intuitively reasonable result if the visual mechanism of the eye functions by detecting differences in the incident luminant energy. According to this

principle, if the contrast degrades by one-half, then the visual area of the target would have to double to restore the detectability to its original level. This can be taken into account in the current model by using an area-contrast product in place of the target visual area. The acquisition rate is then written

$$\lambda = \frac{\beta A}{r^2} \exp\left[\frac{-2.996\ r}{R}\right] \tag{A.2}$$

If we now consider a case in which the target is approaching at a constant rate $\dot{r}$, then the integral of the acquisition rate when evaluated t_2 seconds prior to collision is

$$\int_{t_2}^{\infty} \lambda\ dt = \frac{\beta A}{\dot{r}^2} \int_{t_2}^{\infty} \frac{1}{t^2} \exp\left[\frac{-2.996\ |\dot{r}|}{R} t\right]\ dt \tag{A.3}$$

By substituting $y = t/t_2$ as the variable of integration this can be written

$$\int_{t_2}^{\infty} \lambda\ dT = \frac{\beta A}{\dot{r}^2\ t_2}\ E_2\left[\frac{2.996\ |\dot{r}|t_2}{R}\right] \tag{A.4}$$

where $E_2(z)$ is the second-order exponential integral defined by

$$E_2(z) = \int_1^{\infty} \frac{\exp(-zy)}{y^2}\ dy \tag{A.5}$$

The value of the function $E_2(z)$ can be obtained from the following series expression:

$$E_2(z) = \exp(-z) + 0.57721\ z + z\ \ln(z) + \sum_{n=1}^{\infty} \frac{(-1)^n\ z^{n+1}}{n\ n!} \tag{A.6}$$

The function is plotted in Fig. A.1.

The cumulative probability of visual acquisition for a search that begins at time t_1 and ends at time t_2 can then be written

$$P(acq) = 1 - \exp\left[\frac{-\beta A}{\dot{r}^2}\left(\frac{1}{t_2}\ E_2\left[\frac{2.996\ |\dot{r}|t_2}{R}\right] - \frac{1}{t_1}\ E_2\left[\frac{2.996\ |\dot{r}|t_1}{R}\right]\right)\right] \tag{A.7}$$
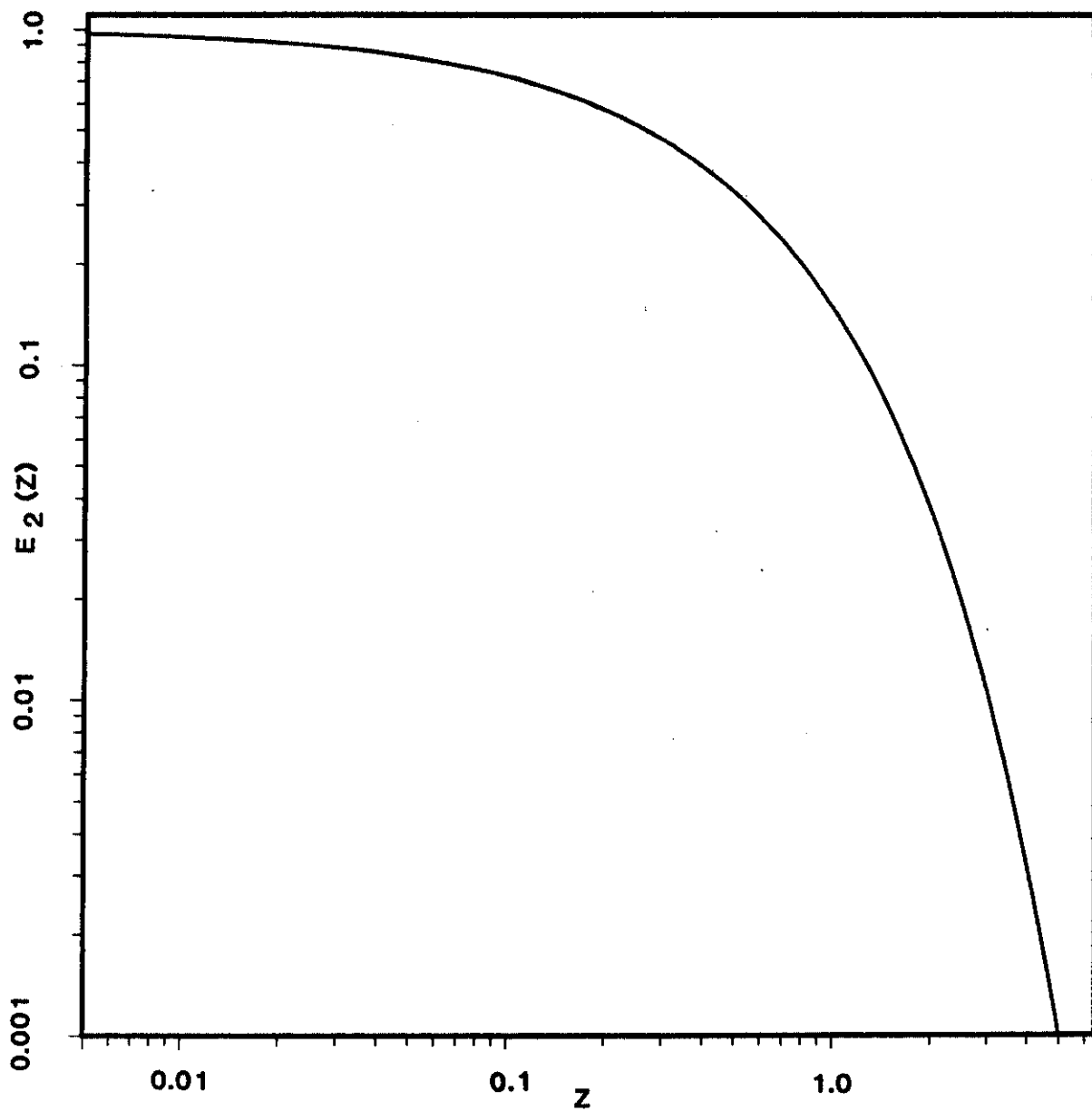
Fig. A.1 The exponential integral E_2 (z).

note that when the contribution of the term containing t_1 is small, then the remaining argument of E_2 in equation (A.7) is proportional to the required visual acquisition range expressed as a fraction of the visual range. In order for visual acquisition to be successful, it is obviously desirable for the required acquisition range to be significantly less than the visual range ($|rt_2| \ll R$).

If equation (A.7) is compared with the corresponding equation for no atmospheric effects (equation 2.9) it can be seen that the function E_2 represents the extent to which atmospheric visibility has decreased the integrated visual acquisition rate. When the atmospheric visibility is unlimited $E_2(0)=1$, and equation (A.7) reduces to equation 2.9.

It should be noted however that the value of β used to fit equation 2.9 to the "good VMC" data is lower than the value that would best fit the more explicit expression (A.7) to the same data. For example, if the "good VMC" conditions under which data was collected were taken to mean 14 miles visual range rather than infinite visual range, then the value of β used to fit the data would increase to 190,000/sec (rather than 130,000/sec).

Another slight refinement is included in the curves that follow. The probability of visual acquisition is set to zero when the angular area subtended by the target is less than that of a circle with diameter of one minute of arc. This reflects the fact that the human eye has a resolution threshold below which a target will never be acquired regardless of the time spent searching. This refinement is not significant if the search does not start until a traffic advisory is received (because then the target usually exceeds the resolution threshold before search begins). However, it can be an important correction in unalerted search since it establishes a lead time at which visual search effectively begins.

Figure A.2 shows the effect of visual range upon the predicted probability of visual acquisition. Nominal single-pilot search is assumed in this figure. It can be seen that for closing rates above 400 knots, a significant degradation in visual acquisition capability can occur even though the visual range is well above the standard 3 nmi minimum for visual flight rules (VFR). Figure A.3 provides similar curves for an increased lead time of 15 seconds. Because acquisition must occur at a longer range, the atmospheric effects are more severe. Figure A.4 provides corresponding curves for two-pilot search and 6 seconds required acquisition time.

Reference

A.1 Jones, D.B., "Air-to-Ground Target Acquisition Source Book: A Review of the Literature," AD-A015 079, Martin Marietta Corp. (30 September 1974).

A.2 Douglas, C.A. and Booker, R.L., "Visual Range" Concepts, Instrumental Determination, and Aviation Applications," NBS Monograph 159, FAA-RD-77-8, National Bureau of Standards, Washington, D.C. (February 1977).
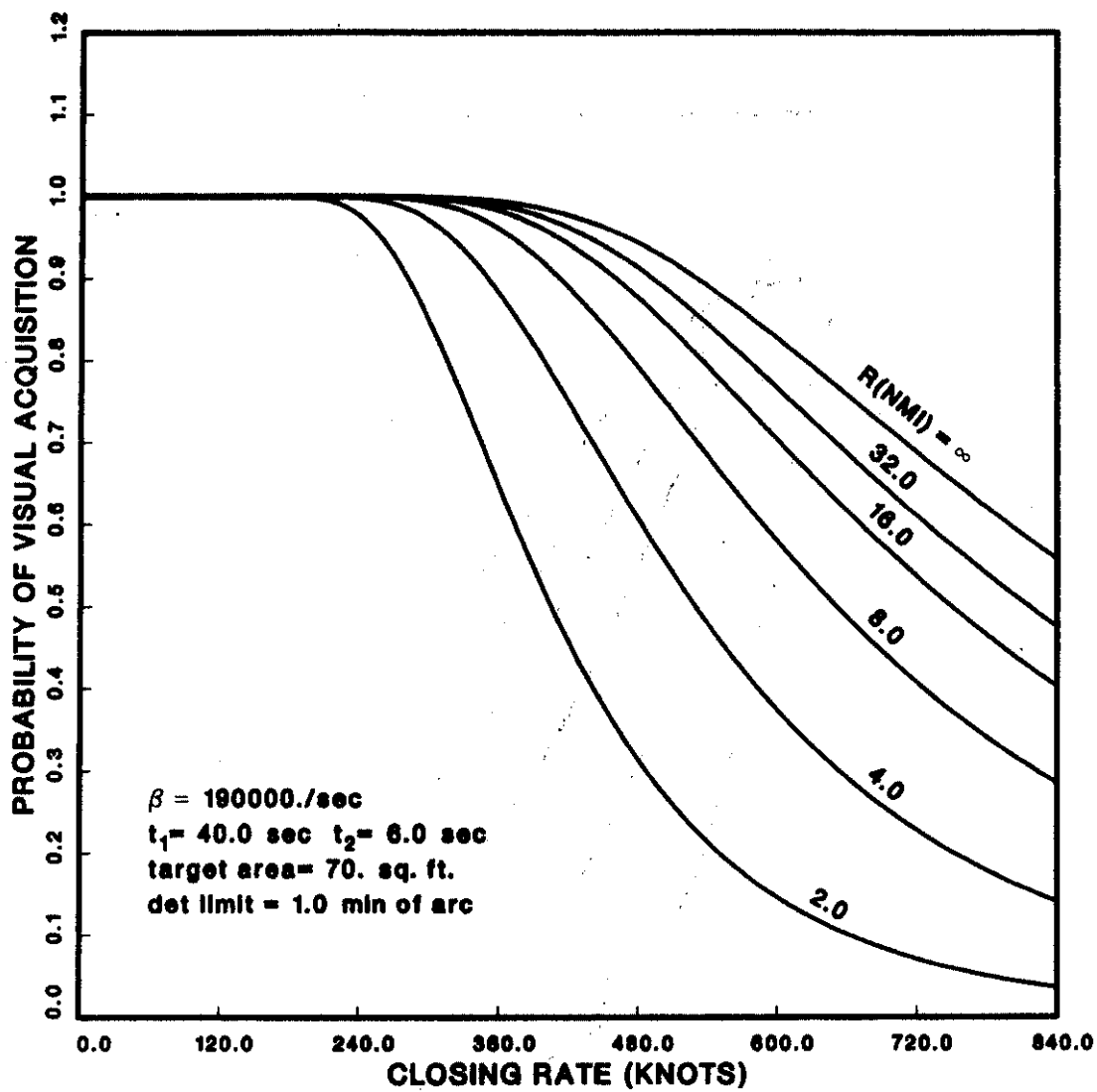
Fig. A.2 Probability of visual acquisition for visual ranges

from 2.0 nmi to infinity. Parameter selections correspond

to single-pilot alerted search and 6 seconds required lead time.
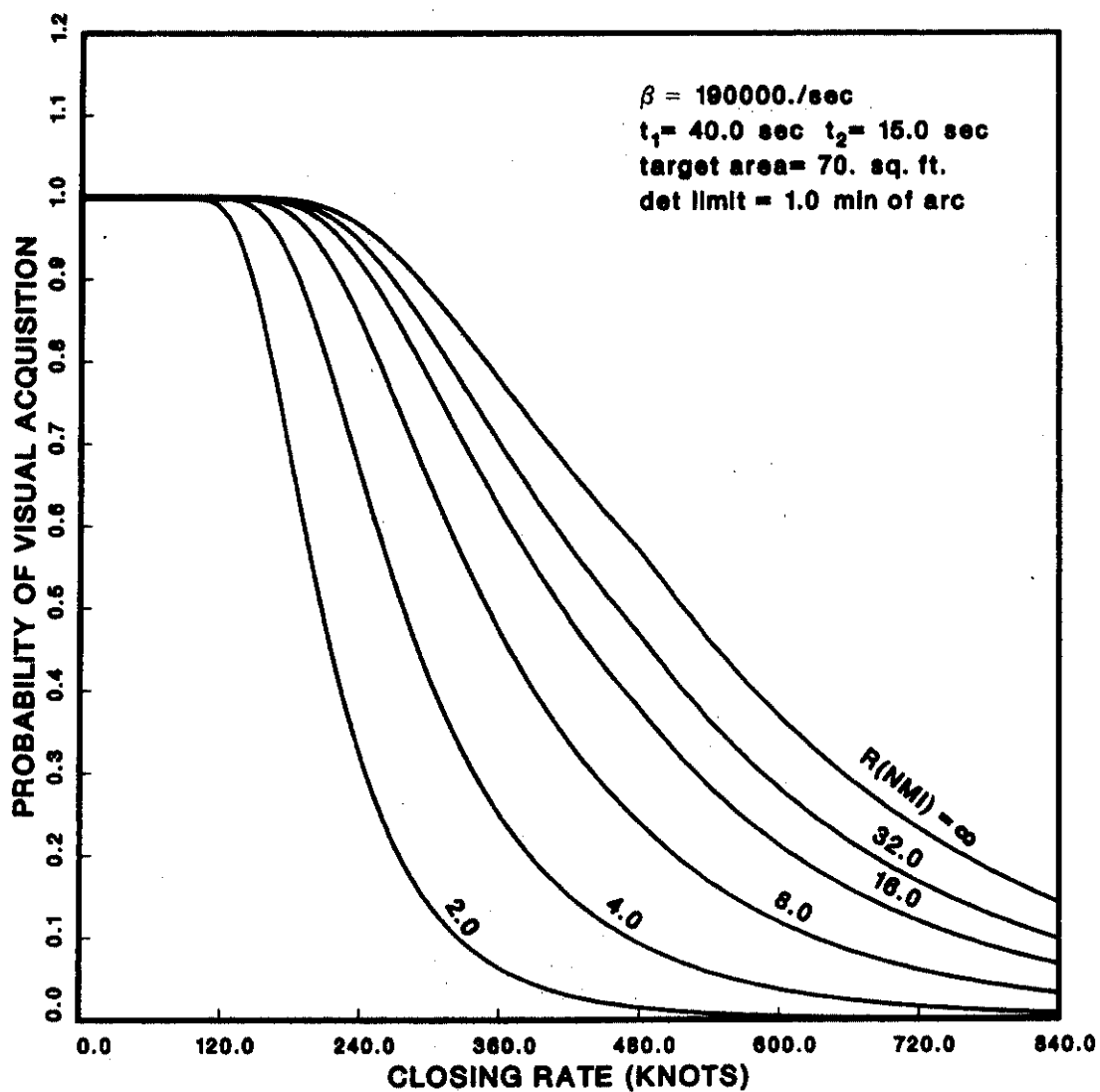
Fig. A.3 Probability of visual acquisition for 15 seconds required lead time. Parameter selections correspond to single-pilot alerted search.
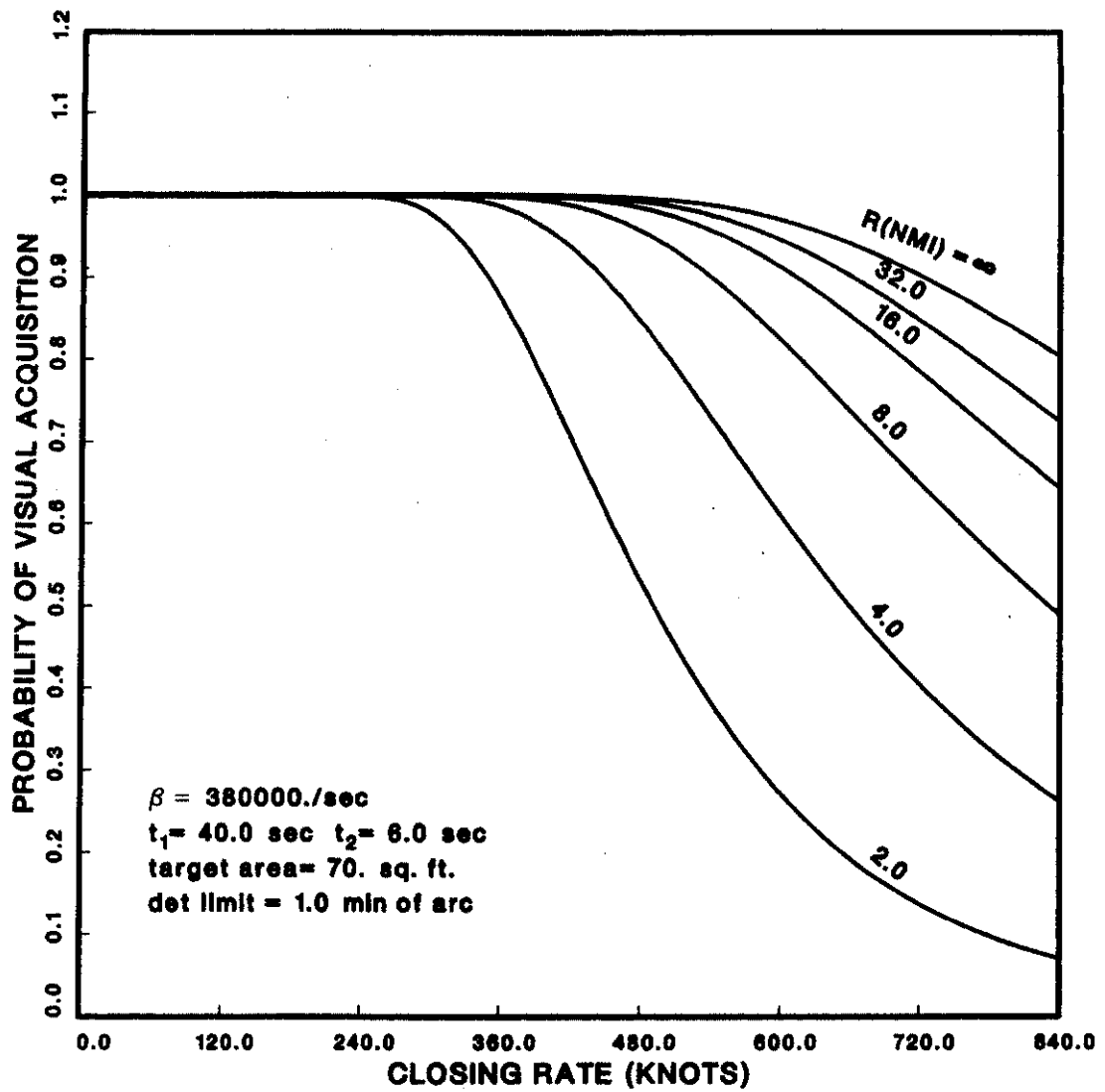
Fig. A.4 Probability of visual acquisition for two-pilot alerted search.
The required lead time is 6.0 seconds.

APPENDIX B

TCAS II FLIGHT TEST DATA

Table B.1 provides the visual acquisition data obtained in TCAS II flight testing at Lincoln Laboratory (Ref. 2). In this testing a subject pilot used an experimental TCAS II installation in a Cessna 421 aircraft during staged encounters with a Beech Bonanza intruder. The subject was asked to fly the aircraft, to use the TCAS traffic advisories and resolution advisories, and to call out all sightings of traffic. A safety pilot accompanied the subject, but did not assist in the search for traffic. This table contains only those encounters in which the intruder approached from the forward hemisphere. This data is the basis of the scatter plot in Fig. 3.1.

The notes in Table B.1 indicate the factors, when known, that contributed to late or missed visual acquisition. Four of the nine cases in which there was no visual acquisition occurred in scenario 22. In this scenario, the TCAS aircraft is descending on final approach with the intruder closing in a head-on geometry from below the TCAS altitude. In this geometry, it is difficult to acquire the intruder before the RA appears since the closing rate is high and the target visual area is small. After the TCAS aircraft began responding to the "climb" resolution advisory, the nose of the Cessna 421 tended to block the line-of-sight to the intruder which was passing below and on the opposite side of the aircraft from the subject pilot.

TABLE B.1.

VISUAL ACQUISITION RESULTS

ENCOUNTER ID. NO.	APPROACH BEARING (CLOCK POSITION)	CLOSING RATE (KT)	RANGE OF ACQUISITION (NMI)	NOTES
20101	12	370	----	Closest approach 1.3 nmi.
20102	1	290	1.00	
20104	12	320	2.30	
20105	11	250	1.10	
20106	2	176	2.10	
20107	1	239	1.40	
20108	11	180	2.50	
20109	10	186	----	Closest Approach 1.2 nmi.
20201	11	175	2.55	
20202	12	240	2.00	
20203	10	90	0.60	Bad ATC advisory confused pilot.
20205	11	240	2.40	
20206	12	250	----	Scenario 22.
20303	1	300	2.20	
20305	12	185	1.80	
20501	2	300	1.02	
20504	12	241	1.40	
20505	12	244	0.83	
20601	1	242	1.80	
20602	10	120	2.40	
20604	11	239	0.50	
20605	1	178	----	Scenario 22.
20606	11	270	3.30	
20608	12	230	2.01	
20703	12	260	2.06	
20704	1	255	2.12	
20705	12	204	3.10	
20706	12	206	2.21	
20707	12	90	1.97	
20801	12	246	1.43	
20802	12	242	2.20	
20803	2	160	1.20	
20804	10	195	1.95	
20805	11	186	2.60	
20806	12	231	----	Scenario 22.

TABLE B.1.

VISUAL ACQUISITION RESULTS (CONT'D)

ENCOUNTER ID. NO.	APPROACH BEARING (CLOCK POSITION)	CLOSING RATE (KT)	RANGE OF ACQUISITION (NMI)	NOTES
20901	12	246	2.20	
20904	10	215	1.42	
20905	12	206	1.00	
21002	11	215	0.90	
20004	12	242	2.25	
21005	10	182	1.10	
21006	10	135	1.60	
21007	12	51	0.85	
21501	12	245	0.79	
21504	11	182	-----	Did not use color coding. Subject concentrated on an altitude-unknown target.
21505	2	180	1.10	
21601	10	265	1.52	
21602	1	180	0.60	Subject misinterpreted display.
21603	11	205	1.40	
21604	11	250	0.50	Scenario 22.
21702	11	240	0.70	Subject stopped search for 10 sec.
21705	9	100	2.00	
21706	12	40	1.40	
21801	11	280	1.00	
21802	11	270	1.10	
21803	2	165	1.50	
21804	11	205	1.30	
21805	11	240	0.91	
21901	11	238	2.20	
21904	11	240	1.10	
21905	11	280	-----	Scenario 22.
22101	1	140	----	Subject stopped searching after RA appeared.
22102	12	230	0.50	
22104	11	220	0.95	
22105	11	240	-----	Closest approach 0.3 nmi.
22107	10	280	2.10	